Measurement method for photoluminescent quantum yields of fluorescent organic dyes in polymethyl methacrylate for luminescent solar concentrators

L. R. Wilson* and B. S. Richards

School of Engineering and Physical Sciences, Heriot-Watt University, Edinburgh, EH14 4AS, UK

*Corresponding author: lrw1@hw.ac.uk

Received 15 July 2008; revised 29 November 2008; accepted 1 December 2008;
posted 3 December 2008 (Doc. ID 98847); published 7 January 2009

A method for measuring the photoluminescent quantum yields (PLQY) of luminescent organic dyes is presented. The self-absorption probability calculated at different dye concentrations is used to determine the absolute quantum yield from the observed values. The results for a range of commercially available dyes show high quantum yields, even at high concentrations, and an absence of quenching. The PLQY of several dye mixtures are also presented. The results indicate an absence of any reduction of PLQY in a dye mixture as compared with the individual PLQY of the dyes. © 2009 Optical Society of America

OCIS codes: 260.2510, 300.6280, 000.2170.

1. Introduction

Luminescent solar concentrators [1–7] (LSCs) provide a means for reducing the area of semiconductors (typically silicon) required to harvest light and convert this into DC electricity in a solar panel. A driving factor in their development is the present high cost of photovoltaic (PV) grade silicon and high demand. Therefore, technologies that reduce the active PV device area, either via a thin-film process or by concentrating sunlight, can potentially achieve cost reduction. LSCs fit into the latter category and typically consist of a plastic sheet made of material such as polymethyl methacrylate (PMMA) doped with luminescent material, such as a fluorescent organic dye. Incident sunlight within the absorption range of the dye is absorbed and the fluorescence is waveguided by total internal reflection toward the edge of the sheet, where it illuminates solar cells optically coupled to the sheet edge. The entire device acts as a concentrator because of the edge/surface area ratio.

While LSCs were first proposed more than 30 years ago [6], one of the major problems that has hindered development has been the lack of fluorescent dyes that exhibit both high quantum efficiencies and good photostabilities. However, a range of visible fluorescent dyes (the BASF Lumogen F series) has been developed specifically for use in LSCs [8]. Previous results from our group indicated that many of the dyes have near-100% quantum yields [9]. To determine their suitability for use in LSCs, the absorption spectrum, emission spectrum, and quantum yield of each of the Lumogen dyes have been measured over a range of different concentrations. We present a new technique that has been developed for accurately determining the photoluminescent quantum yields (PLQY) of five of the Lumogen dyes based on the progression of measured PLQY as the concentration of the dyed sample (and, hence, the self-absorption probability) is increased. The method and results presented here demonstrate the high PLQY of the Lumogen dyes and also exhibit an absence of quenching at high concentrations in some of the dyes.

0003-6935/09/020212-09$15.00/0

Although individual dyes have high PLQY, they only absorb a narrow range of wavelengths (typically ~100 nm). To absorb a wider range of wavelengths and make better use of the solar spectrum incident on an LSC, a mixture of several different dyes is normally used [10]. The results presented here also demonstrate that the individual dyes still have high PLQY when combined in a dye mixture.

2. Background

Traditionally, the PLQY of liquid samples has been measured using a spectrofluorometer by comparison with a quantum yield standard [11–13]. In this method, the absorbance and fluorescence emission intensity from a progression of different concentrations of both the compound under study and the PLQY standard are measured. The PLQY of the sample can be calculated from the variations of fluorescence intensity with increasing absorbance. However, this technique is limited to liquid samples (solid samples present scattering problems, as described later) and is also limited by the need for a PLQY standard with known quantum yield, absorption, and fluorescence spectra [11–13]. For solid samples, two other techniques have been used previously. The first, the thermal-lens (TL) technique [14–20], is based on measuring the amount of heat deposited in a sample by the amount of excitation light that is absorbed. A large amount of deposited heat indicates a low quantum yield (the absorbed excitation light is turned into heat instead of fluorescence emission). However, this method can only be used on sheet samples that have good, optical-quality surfaces and low scattering. In addition, since no standard thermal-lens system exists, it is difficult to repeat or compare results obtained on different systems.

A major challenge with measuring the PLQY of solid samples is the possible presence of scattering within the sample. This will scatter both the incident excitation light and the fluorescence emission. The angular distribution of absorbance and fluorescence will depend on the sample geometry and is impossible to predict. To overcome this problem, the second technique uses an integrating sphere to average the fluorescence emission over all angles. When used with a photon-counting spectrofluorometer, the PLQY can be easily determined from the areas of the emission and excitation spectra. The accuracy of this method is usually quoted as 10%. However, as is shown here, it is possible to use the progression of measured PLQY with increasing sample concentration to calculate the actual PLQY. The repeatability of the integrating sphere method is better than 2% (measured later). There are several important advantages to the integrating sphere method. Since commercially available integrating spheres are used, results are easily repeatable between experimental setups. There are few restrictions on the samples that can be used in the sphere (liquid, solid, powder) or on their optical quality (e.g., surface roughness or scattering). Even though the emission of light from the sample may not be isotropic, the sphere provides an output that is averaged over all sample emission angles. Therefore, it should be possible to measure rough and scattering samples with equal success.

3. Theoretical

The absorption coefficients of the various dyes are calculated from the fractional transmittances of both a clear sample of PMMA and samples containing the dyes under study. The dye absorption coefficient described here is the Napierian coefficient, derived from the *natural* logarithm of the ratio of the transmitted and incident intensities [21]. For a dye concentration in parts per million (ppm) and a path length in centimeters, the absorption coefficient has units of $\mathrm{ppm}^{-1}\,\mathrm{cm}^{-1}$.

Before the absorption coefficient can be calculated, corrections must be applied for the surface reflectivity of the samples. The reflectivity is calculated from the PMMA refractive index. This, in turn, is calculated from the Cauchy coefficients [22] for PMMA, using

$$n = A + \frac{B}{\lambda^2} + \frac{C}{\lambda^4}, \tag{1}$$

where the coefficients, for λ in nanometers, were measured as

$$\begin{aligned} A &\quad 1.48763, \\ B &\quad 3230.8581, \\ C &\quad 121652590.8071, \end{aligned}$$

which are in agreement with published values for PMMA [23]. The samples used for refractive index measurement were of commercial PMMA containing UV stabilizer and were made by Lucite International using a standard thermal polymerization technique [24]. Although the Cauchy equation is not accurate in the UV region [22], the error introduced when it is used for calculating interface transmittance is minimal. A 5% error (which may be typical in the UV) in refractive index translates to only a 1% error in transmittance.

In case the addition of the fluorescent dye had an effect on the refractive index of the sample and, hence, the surface reflectivity, samples of both clear PMMA and PMMA dyed with 1000 ppm of Rot 305 were measured using a Metricon prism refractometer. The indices obtained were 1.496 and 1.499, respectively. These are identical to within the experimental error of the equipment.

To eliminate the presence of scattering in the samples, the transmission of samples of clear and dyed PMMA were measured in a region where the dye has negligible absorption. The Violett 570 dye was used in a concentration of around 500 ppm and the samples were measured in the range of 500–600 nm. The transmission for both clear and dyed was 92%, which indicates the only loss is due to reflection from the front and rear surfaces of the sample. A sample

refractive index of 1.5, which was measured at this wavelength, accounts for the remaining 8%.

Once the absorption spectrum of the dye has been measured, a suitable excitation wavelength can be chosen and the PLQY determined using the integrating sphere. The sample is excited with monochromatic light. The numbers of photons absorbed and emitted by the sample are calculated from the areas of excitation and emission spectra recorded both with and without the sample in the sphere. The "emission" spectrum with the empty sphere gives a background spectrum, which accounts both for detector dark counts and any emission from the sphere itself (e.g., Raman).

The four spectra are designated as below (E, emission; L, excitation; A, empty sphere; C, sample present):

emission spectrum, sample in sphere E_C;
excitation spectrum, sample in sphere L_C;
excitation spectrum, empty sphere L_A; and
emission spectrum, empty sphere E_A.

The PLQY is calculated from

$$\mathrm{PLQY} = \frac{E_C - E_A}{L_A - L_C}, \tag{2}$$

where E_C, E_A, L_A, and L_C are the areas of the respective spectra. The areas are calculated from the raw spectral data by summing the product of photon count rate and wavelength over the entire spectrum; for example $E_C = \sum E_C(\lambda)\Delta\lambda$, where E_C is the area of the emission spectrum and $E_C(\lambda)$ is the photon count rate at a particular wavelength.

When the fluorophore has a small Stokes shift, as is the case with the Lumogen F dyes, there is a high probability that the fluorescence photon will be reabsorbed by the sample. The same PLQY will apply to reabsorption/reemission events. This will lead to an apparent reduction in the measured PLQY of the sample, especially of samples with low quantum yields. Two different kinds of self-absorption can occur. First, fluorescence photons that are trapped within the integrating sphere (but outside the sample) can pass through the sample multiple times and be reabsorbed by another dye molecule in the sample. Second, fluorescence photons emitted from within the sample can be reabsorbed before they have a chance to reach the sample's surface. The second process is more important in highly concentrated samples, while the first dominates for low concentrations. Although the two situations are different, the effect they have on the measured PLQY can be treated similarly.

The integrating sphere is shown in Fig. 1. Ray 1 represents the excitation light. Ray 2 denotes fluorescence emission that has left the sample and is inside the sphere but that passes back through the sample and becomes reabsorbed. Ray 3 shows fluorescence emission being absorbed inside the sample,

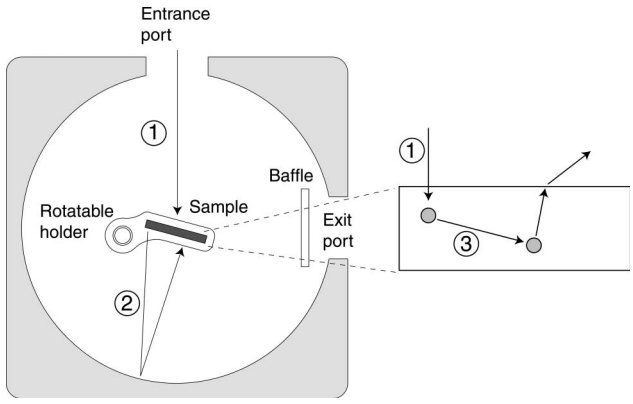

Fig. 1. Integrating sphere and self-absorption mechanisms. 1 Excitation light. 2 Fluorescence light reabsorbed by sample. 3 Fluorescence light internally reabsorbed by sample.

before the primary emission reaches the surface of the sample and escapes.

As self-absorption increases, the observed emission spectrum will be increasingly red shifted. However, the shape of the emission spectrum in the long-wavelength regime, where the dye absorption is negligible, will show minimal difference compared with the molecular emission spectrum. It has been shown that there can be an absorption "tail" of extremely low absorption coefficient that extends several hundred nanometers after the bulk of the dye absorption spectrum [25]. Although the amount of the tail is minimal (around 0.1% absorption in a 2 mm sample for the dye studied [25]), the large number of absorption/emission events that can occur in the integrating sphere may lead to a difference in the observed emission spectrum in the long-wavelength region and a consequent error in the self-absorption correction needs to be applied.

The self-absorption correction used here is based on that described by Ahn *et al.* [26]. Using this technique, the molecular emission spectrum (measured from a dilute sample that is not affected by self-absorption, typically a concentration of a few ppm) is scaled to match the observed emission spectrum at long wavelengths. This is shown in Fig. 2. Both the absorption spectrum and molecular emission spectrum (obtained from a weakly doped sample outside the sphere) are plotted and these are mirror images of each other, as would be expected. However, the *observed* emission spectrum from the sample inside the sphere is red shifted because of the multiple absorption/reemission events that occur inside the sphere. It is *not* a mirror image of the absorption spectrum for this reason. The molecular emission has been scaled to match the observed emission at wavelengths greater than ~575 nm, where self-absorption is negligible.

It can be seen in Fig. 2 that, although the absorption spectrum appears only to extend to around 520 nm, there is still a difference in the molecular emission and observed emission spectrum up to

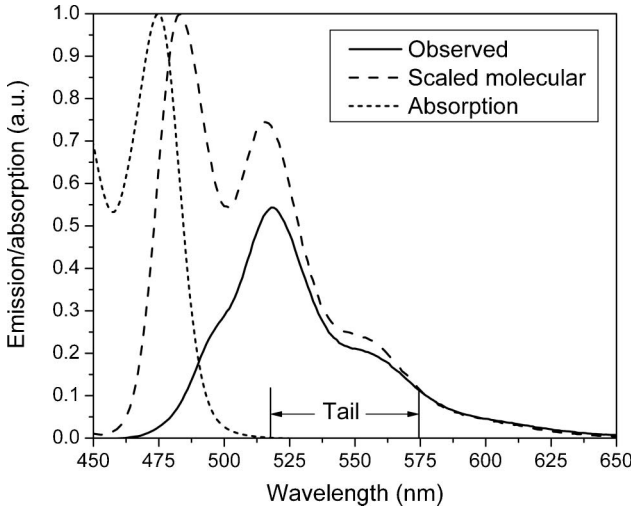

Fig. 2. Scaling of the molecular emission spectrum.

575 nm, an indication of an absorption tail extending at least to 575 nm.

Denoting the scaled molecular emission spectrum by $F'(\lambda)$ and the observed emission spectrum by $F_{\text{obs}}(\lambda)$, a self-absorption coefficient (SA coefficient), a, can be calculated from

$$a = 1 - \frac{\sum F_{\text{obs}}(\lambda)\mathrm{d}\lambda}{\sum F'(\lambda)\mathrm{d}\lambda}. \tag{3}$$

Both $F'(\lambda)$ and $F_{\text{obs}}(\lambda)$ are measured in terms of photon count rate as before. a can take values ranging from 0 (zero self-absorption) to 1 (maximum self-absorption). The corrected PLQY can then be calculated from the observed PLQY by using

$$\text{PLQY}_{\text{corr}} = \frac{\text{PLQY}_{\text{obs}}}{1 - a + a\text{PLQY}_{\text{obs}}}. \tag{4}$$

As can be seen from Eq. (4), if the real quantum yield is 1.0, then self-absorption will have no effect on the measured value.

When the excitation spectrum is recorded, a neutral density filter (typically 0.5% transmission) must be inserted between the sphere and the detection monochromator because the much higher intensity of the excitation would damage the photomultiplier detector if it were not reduced. The transmittance of the filter is measured *in situ* and is used to scale the excitation spectrum used in the calculations. Since the number of absorbed photons is calculated from the difference in the areas of the excitation spectrum with and without the sample in the sphere, it is necessary to have a sufficient number of photons absorbed to make this calculation accurate. This excludes the measurement of weakly absorbing samples. Typically, a minimum sample absorbance of 0.1 (at least 20% absorption) is required.

Quenching of the sample fluorescence, i.e., a reduction in dye PLQY, may occur at high dye concentrations [12]. In the PMMA samples, the only quenching mechanism likely is concentration dependent, that is, formation of nonfluorescent dimers or polymers of the dye molecules.

The PLQY can, in theory, be determined from a single measurement and self-absorption correction. However, when the PLQY is near 100%, an additional technique can be used to verify the actual PLQY. If there is no quenching present in the sample at higher concentrations, then any decrease in measured PLQY must be due entirely to nonunity PLQY and the effects of self-absorption. The presence or absence of quenching in the sample can be determined by looking at the progression of corrected PLQY values as the dye concentration increases, where a decrease in corrected PLQY indicates quenching. We can determine how much of a decrease in measured PLQY would be expected for a particular increase in the self-absorption coefficient. For example, if a dye has an actual PLQY of 99% and a self-absorption coefficient of 0.7 is measured, the observed PLQY will drop to 96.5%, a decrease of 2.5%. If the observed decrease in measured PLQY is less than this, we can be confident that the actual PLQY lies between 99% and 100%. Since the repeatability of the integrating sphere technique is of the order of 2%, we can then achieve an accuracy of around 1% when the PLQY lies near 100%.

4. Experimental

A. Preparation of Samples

Samples of PMMA containing the Lumogen dyes in varying concentrations were cast using a standard thermal polymerization technique [24]. The final sheet thickness was around 3 mm. No additives, such as UV stabilizers or cross-linking agents, were used in these samples (unlike the samples for refractive index measurement, which were commercial and contained UV absorber). The residual monomer content of the sheet was less than 0.3 wt. %(determined by gas chromatography). Samples of the sheets were used directly for the fractional transmittance measurements. To prepare samples suitable for the integrating sphere, disks (11 mm diameter by 1.9 mm thick) were turned from the sheet using a lathe.

Although free radicals are present in the polymer during polymerization, they do not appear to have any detrimental effects on the performance of the dyes. Several of the dyes (Orange 240, Gelb 083) were measured in the monomer itself before polymerization and gave exactly the same quantum yields as after polymerization. It is, therefore, unlikely that the dyes are damaged by the radicals present.

B. Measurement of Fractional Transmittance

A standard UV-visible spectrophotometer (Shimadzu GC90-UV) was used. A baseline scan was first run with an empty sample compartment. The fractional transmittance was then recorded with the sample under study in place. Corrections were then applied

for the sheet reflectance and host absorption as described previously.

C. Measurement of Molecular Fluorescence Spectrum

To avoid self-absorption distorting the measured fluorescence spectrum, an extremely weakly doped sample was used (typically a concentration of ~2 ppm by weight). The disc samples made for the integrating sphere were used. A Horiba Jobin–Yvon Fluoromax 3 spectrofluorometer was used to excite the sample and collect the fluorescence emission. The sample was mounted directly in the sample compartment of the instrument. The integrating sphere is not used for this measurement. As an additional precaution against self-absorption effects, the sample was only excited at a small region close to the edge and the fluorescence was collected from the same region, as shown in Fig. 3.

The weak dye concentration, combined with the extremely short path length of the fluorescence light, makes the effect of self-absorption negligible. As is shown in Fig. 3, only the emission directed to the right is collected, as it will be free of self-absorption. The emission to the left (from the opposite end of the sample) is discarded, as it will be affected by self-absorption because of the much longer path length through the sample.

In the spectrofluorometer, there is a reference detector to measure the excitation light intensity. This is used to correct for any variations in lamp intensity that might occur over the course of a measurement.

D. Measurement of Photoluminescent Quantum Yields

The standard Jobin–Yvon integrating sphere accessory was used with the Fluoromax 3 spectrofluorometer to record quantum yields. It is made from Spectralon and has an internal diameter of 100 mm and port diameters of 20 mm, giving a port/sphere area ratio of 2%. The sphere can accept either solid (11 mm diameter disc) or liquid (5 mm silica cuvette) samples. The sample is mounted at the focal point of the excitation light. Dimensions of the excitation beam at the focus are approximately 2 mm × 10 mm, depending on the excitation slit setting. The sample can be pivoted in its holder to orient it relative to the excitation beam. For solid samples, the sample is angled at ~15° to the input beam so that specularly reflected excitation light is directed toward the wall of the sphere, rather than back out the entrance port.

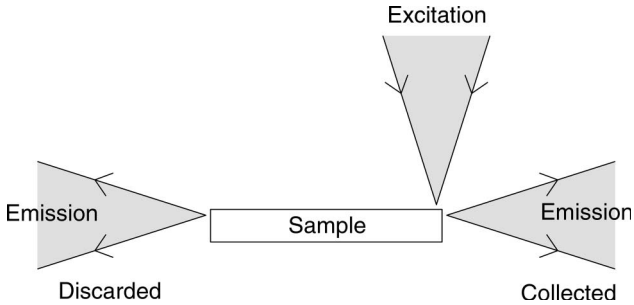

Fig. 3. Measurement of sample fluorescence.

A Spectralon baffle is mounted over the exit port to prevent fluorescence from reaching the detector directly. To establish the accuracy of the method, both quinine sulphate and Rhodamine 101 samples were measured in the integrating sphere. PLQYs of 57% and 98%, respectively, were obtained, which are in excellent agreement with literature values [11–13]. An Excel spreadsheet is used to calculate the areas of the spectra and compute the quantum yield.

5. Results

A. Dye Absorption and Emission Spectra

The transmittance spectra of the sheets of dyed PMMA were used to calculate the mass absorption coefficient, as described in Section 3. A clear (undoped) PMMA sheet was used to correct for the PMMA absorption and the Cauchy equation used to correct for the surface reflectivity. The fluorescence spectra were measured using the Fluoromax as described.

The dye absorption coefficient was measured using samples with a high enough concentration of dye to give a detectable absorption, but not so high as to transmit so little light as to make detection impossible. Dye concentration was chosen to give around 70%–90% peak absorption in a ~3 mm thick sample. For measurement of the molecular emission spectrum, it is necessary to use an extremely weakly doped sample to avoid (or at least minimize) the effects of self-absorption within the sample on the fluorescence emission. Samples chosen for emission measurement were typically of 2–3 ppm concentration. The dye absorption spectrum will not depend on concentration, so it is acceptable to use different dye concentrations for the two measurements. The actual concentrations used are shown in Table 1.

The absorption and emission spectra are plotted in Fig. 4. Absorption spectra are in units of $ppm^{-1}\,cm^{-1}$ and are normalized to 1. Emission spectra are in units of counts per second (cps) and are also normalized to 1. Absorption and emission spectra are mirror images of each other, as would be expected.

Features of the absorption and emission spectra are listed in Table 2. The average emission wavelength was calculated by integrating the emission spectrum of each dye.

As a result of the wide range of absorption wavelengths, it is possible to absorb all of the solar radiation from 350 up to 620 nm by using a combination of several of the dyes.

Table 1. Sample Concentrations

Dye	For Absorption (ppm)	For Emission (ppm)
Violett 570	65	3.5
Gelb 083	35	1.7
Gelb 170	35	1.8
Orange 240	25	1.2
Rot 305	70	3.5

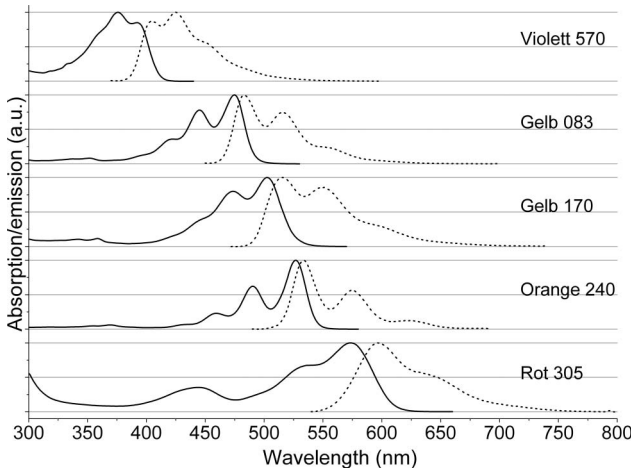

Fig. 4. Absorption (solid curve) and emission (dotted curve) spectra. Spectra offset vertically for clarity.

B. Dye Quantum Yields

The uncorrected PLQY, self-absorption coefficient, and corrected PLQY will be presented separately for each dye. The self-absorption correction only has significance when the dye has a PLQY of less than 100%. For this reason, the corrected PLQY is only shown for those dyes with nonunity PLQY.

1. *Repeatability*

The repeatability of the integrating sphere method was checked by running ten experiments on the same sample. Measurements were split over two days. The sample holder was also rotated slightly (~5°) halfway through the measurements to see if the angular position of the sample had any effect on the measured PLQY. The spread of measured PLQY values was no greater than 2% over all the readings, therefore, 1% error bars are shown on the PLQY graphs. Additionally, the change in orientation of the sample holder had no effect on the readings.

2. *Violett 570*

An excitation wavelength of 370 nm was chosen. Although this excites the dye effectively, it is also absorbed by the PMMA host material. In order to compensate for this, a sample of clear (undoped) PMMA was used in the sphere when the "empty sphere" spectra were recorded. Because the undoped reference sample had exactly the same dimensions as the dyed sample, the absorption of the PMMA should be effectively corrected for. The PLQY and the self-absorption coefficient are shown in Fig. 5.

As the dye concentration is increased, the amount of self-absorption (as measured by the self-absorption coefficient) increases, as expected. However, there is no apparent decrease in the PLQY, despite this increased self-absorption. Because there is no decrease in measured PLQY, no quenching is occurring at higher concentrations. Additionally, the actual dye PLQY must be between 99% and 100%, as a lower value would lead to a drop of the measured PLQY as self-absorption increases.

3. *Gelb 083*

An excitation wavelength of 440 nm was used. The PLQY and the self-absorption coefficient are shown in Fig. 6. The PLQY shows a decrease with increasing dye concentration; however, this is purely due to increased self-absorption, as the corrected PLQY does not change with increasing concentration. No quenching occurs at the higher dye concentrations. The PLQY is $96\% \pm 1\%$.

4. *Gelb 170*

An excitation wavelength of 460 nm was used. The PLQY and the self-absorption coefficient are shown in Fig. 7. The PLQY is $98\% \pm 1\%$ at low concentrations and shows a slight decrease as the concentration is increased to 790 ppm. This is evidence of quenching at the higher concentrations.

5. *Orange 240*

An excitation wavelength of 480 nm was used. The PLQY and the self-absorption coefficient are shown in Fig. 8. There is no discernable decrease in the PLQY as the dye concentration is increased. There is, therefore, no quenching. The PLQY is 100%.

6. *Rot 305*

The excitation wavelength was 530 nm. The PLQY and the self-absorption coefficient are shown in. Again, no decrease in PLQY is observed, despite the increase in dye concentration and self-absorption coefficient. This indicates both 100% PLQY and an absence of quenching. PLQY and self-absorption coefficient are shown in Fig. 9.

Table 2. Spectral Features

Dye	Peak Absorption λ (nm)	Peak Absorption Coefficient ($ppm^{-1}\,cm^{-1}$)	Peak Emission λ (nm)	Average Emission λ (nm)
Violett 570	376	0.1125	425	434
Gelb 083	475	0.2395	483	513
Gelb 170	502	0.1981	516	551
Orange 240	527	0.2291	534	561
Rot 305	574	0.1024	597	622

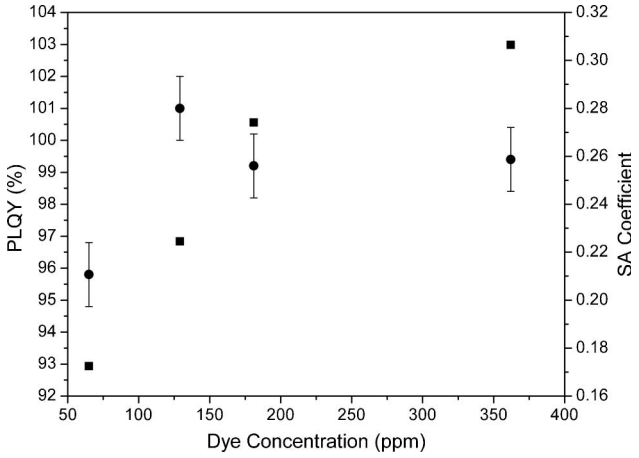

Fig. 5. Violett 570 properties. Measured PLQY (circles) and self-absorption coefficient (squares).

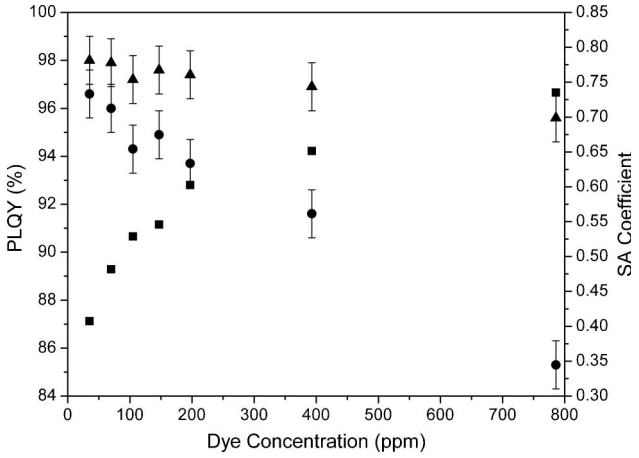

Fig. 7. Gelb 170 properties. Measured PLQY (circles), corrected PLQY (triangles), and self-absorption coefficient (squares).

C. Mixed-Dye Properties (Emission and Photoluminescent Quantum Yields)

The PLQY of samples containing mixtures of both three and four of the Lumogen dyes was measured. The concentrations of the dyes in each of the samples is shown in Table 3.

The emission spectra of the dye mixtures were obtained from the spectra taken from the integrating sphere PLQY measurements. Because of the high reabsorption that occurs inside the sphere and inside the sample, the observed emission spectra were identical to the spectra from the individual dye with the longest emission (Orange 240 for the three-dye mix, Rot 305 for the four-dye mixture), even when the mixture is excited at a short wavelength. For example, when the sample is excited with 380 nm light, only the Violett 570 dye will initially be excited. However, its emission will subsequently be absorbed by the Gelb 083, Orange 240, and Rot 305 dyes. The spectrum which is actually observed will be no different from the Rot 305 emission spectrum. Since some of the dyes have nonunity PLQY, the observed PLQY of the mixture is expected to decrease with shorter excitation wavelengths as more dye interactions will occur. This is observed in practice.

The PLQY of the dye mixtures is shown in Table 4 at different excitation wavelengths. The self-absorption correction has not been applied to the dye mixture results because, unlike for a single dye, the "molecular" emission spectrum (i.e., that observed at low concentrations of the dye mixture) will depend on the excitation wavelength.

Since the spectrometer had to be scanned up to 800 nm to detect all of the Rot 305 emission, it was not possible to excite the four-dye sample with a wavelength shorter than 400 nm, as this would lead to a second-order detected signal. It was, therefore, not possible to excite the violet dye in the four-dye mixture.

The three-dye mixture shows an unusual progression in PLQY as the excitation wavelength is decreased. The high PLQY when excited at 480 nm is easily explained: only the Orange 240 dye is excited at this wavelength and this has unity quantum yield as described in Subsection 5.B. The drop to 97% when excited at 430 nm is because the Gelb 083 dye is now being excited. Since this dye only has a 96% PLQY,

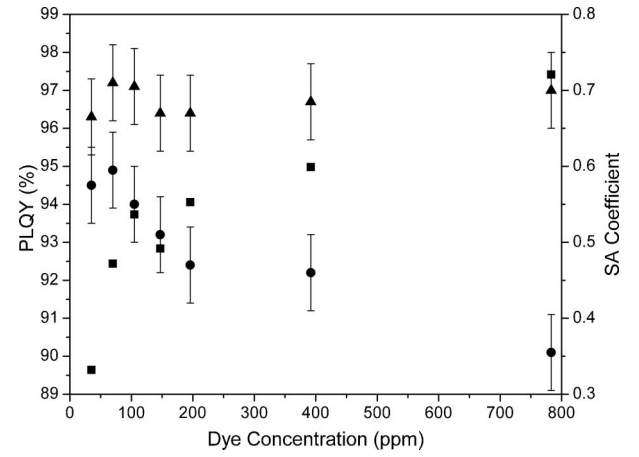

Fig. 6. Gelb 083 properties. Measured PLQY (circles), corrected PLQY (triangles), and self-absorption coefficient (squares).

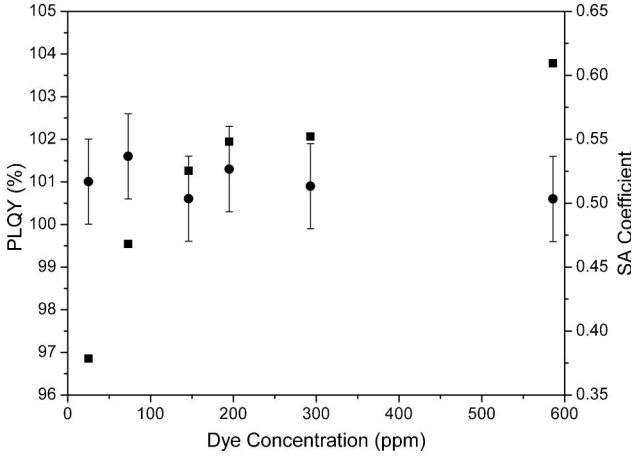

Fig. 8. Orange 240 properties. Measured PLQY (circles) and self-absorption coefficient (squares).

Table 3. Mixed-Dye Concentrations

Dye	Three-Dye Concentrations (ppm)	Four-Dye Concentrations (ppm)
Violett 570	362	362
Gelb 083	196	196
Orange 240	146	146
Rot 305	—	394

the measured PLQY of the mixture drops. The rise in PLQY when the excitation wavelength drops to 380 nm is not easily explained. In theory, it should stay at around 97% as the violet dye has 100% PLQY. The increase is perhaps explained by the emission from the violet dye directly exciting the orange dye, rather than being absorbed by the yellow. Since both the violet and orange have near 100% PLQYs, the measured PLQY will also be near 100%.

The progression of measured PLQY for the four-dye mixture is expected. As the excitation wavelength is decreased, the fluorescence emission is absorbed and reemitted by an increasing number of dyes in the mixture. Since some have less than unity PLQY, the overall PLQY decreases as the excitation wavelength is decreased.

6. Conclusions

The Lumogen F fluorescent dyes have both high (near 100%) quantum yields and cover a wide range of absorption wavelengths in the visible spectrum. With the exception of the Gelb 170 dye, no evidence of appreciable quenching is observed even at concentrations, in some cases as high as 1000 ppm. Combined with their ease of incorporation into PMMA, these dyes appear an excellent choice for luminescent solar concentrators.

Work is currently under way to study the UV stability and weathering of the dyes in PMMA hosts, as this is a major factor in their application in luminescent concentrators. Ray-tracing simulations are also being carried out to determine the most suitable concentration of dye, or a dye mixture, to give the highest overall efficiency for a luminescent concentrator module.

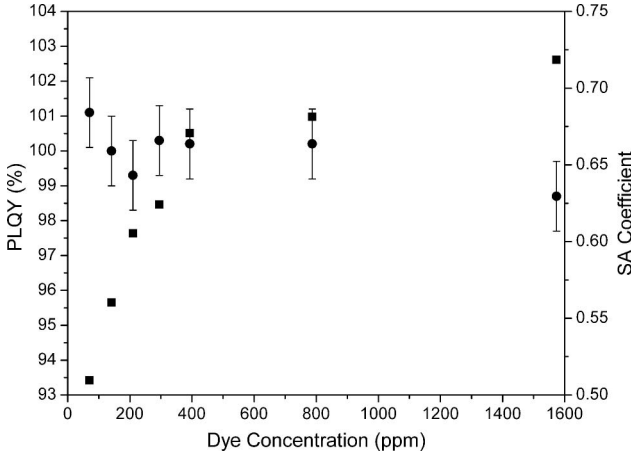

Fig. 9. Rot 305 properties. Measured PLQY (circles) and self-absorption coefficient (squares).

Table 4. Mixed-Dye PLQY

Dye mixture	Excitation Wavelength (nm)	Measured PLQY (%)
Three-dye	480	101%
Three-dye	430	97%
Three-dye	380	104%
Four-dye	530	99%
Four-dye	490	96%
Four-dye	440	92%

The authors thank Neil Kirtley and Lesley Minto of Lucite International (Wilton, UK) for PMMA sheet casting and Patricia Richardson and Anita Jones of the Chemistry Department, Edinburgh University (Edinburgh, UK) for use of the spectrofluorometer facility. The authors are grateful to BASF (Ludwigshafen, Germany) for supplying the Lumogen F dyes used in this research.

References

1. J. S. Batchelder, A. H. Zewail, and T. Cole, "Luminescent solar concentrators. 1: Theory of operation and techniques for performance evaluation," Appl. Opt. **18**, 3090–3110 (1979).
2. J. S. Batchelder, A. H. Zewail, and T. Cole, "Luminescent solar concentrators. 2: Experimental and theoretical analysis of their possible efficiencies," Appl. Opt. **20**, 3733–3754 (1981).
3. A. Goetzberger and W. Greubel, "Solar energy conversion with fluorescent collectors," Appl. Phys. **14**, 123–139 (1977).
4. A. Goetzberger, "Fluorescent solar energy collectors: operating conditions with diffuse light," Appl. Phys. **16**, 399–404 (1978).
5. A. Goetzberger and O. Schirmer, "Second stage concentration with tapers for fluorescent solar collectors," Appl. Phys. **19**, 53–58 (1979).
6. W. H. Weber and J. Lambe, "Luminescent greenhouse collector for solar radiation," Appl. Opt. **15**, 2299–2300 (1976).
7. B. Rowan, L. Wilson, and B. S. Richards, "Advanced concepts for luminescent solar concentrators," IEEE J. Select. Top. Quantum Electron. 14, 1312–1322 (2008).
8. G. Seybold and G. Wagenblast, "New perylene and violanthrone dyestuffs for fluorescent collectors," Dyes Pigments **11**, 303–317 (1989).
9. L. R. Wilson, B. S. Richards, A. C. Jones, P. R. Richardson, A. Cole, Ian Fraser, N. Kirtley, and L. Minto, "Quantum yield measurements of high-efficiency dyes for luminescent solar concentrators," presented at the 4th Photovoltaic Science Application and Technology Conference, Bath, UK, 2–4 April 2008.
10. B. S. Richards and K. R. McIntosh, "Ray-tracing simulations of luminescent solar concentrators containing multiple luminescent species," in *21st European Photovoltaic Solar Energy Conference* (WIP Renewable Energies, 2006), pp. 185–188.
11. "Fluorescence quantum yield standards," http://www.iss.com/resources/yield.html.
12. J. R. Lakowicz, *Principles of Fluorescence Spectroscopy*, 2nd ed. (Kluwer Academic/Plenum, 1999).
13. D. Magde, G. E. Rojas, and P. Seybold, "Solvent dependence of the fluorescence lifetimes of xanthene dyes," Photochem. Photobiol. **70**, 737–744 (1999).
14. J. H. Brannon and D. Magde, "Absolute quantum yield determination by thermal blooming. Fluorescein," J. Phys. Chem. **82**, 705–709 (1978).
15. K. L. Jansen and J. M. Harris, "Double-beam thermal lens spectrometry," Anal. Chem. **57**, 2434–2436 (1985).

16. A. Kurian, K. P. Unnikrishnan, T. S. Lee, V. P. N. Nampoori, and C. P. G. Vallabhan, "Realization of optical logic gates using the thermal lens effect," Laser Chem. **20**, 81–87 (2002).
17. A. Kurian, "Characterization of photonic materials using thermal lens technique," Ph.D. disseration (Cochin University of Science and Technology, 2002).
18. M. L. Lesiecki and J. M. Drake, "Use of the thermal lens technique to measure the luminescent quantum yields of dyes in PMMA for luminescent solar concentrators," Appl. Opt. **21**, 557–560 (1982).
19. S. M. Lima, A. A. Andrade, R. Lebullenger, A. C. Hernandes, T. Catunda, and M. L. Baesso, "Multiwavelength thermal lens determination of fluorescence quantum efficiency of solids: application to Nd^{3+}-doped fluoride glass," Appl. Phys. Lett. **78**, 3220–3222 (2001).
20. V. Pilla, D. T. Balogh, R. M. Faria, and T. Catunda, "Thermal-lens study of thermo-optical and spectroscopic properties of polyaniline," Rev. Sci. Instrum. **74**, 866–868 (2003).
21. J. W. Verhoeven, "Glossary of terms used in photochemistry," Pure Appl. Chem. **68**, 2223–2286 (1996).
22. F. L. Pedrotti and L. S. Pedrotti, *Introduction to Optics*, 2nd ed. (Prentice-Hall, 1993).
23. MicroChem, "NANOTM PMMA resist," http://www.microchem.com/products/pdf/PMMA_Data_Sheet.pdf.
24. R. Vieweg and F. Esser, *Kunststoff-Handbuch Bd. IX Polymethacrylate* (Hanser Verlag, 1975), Vol. IX.
25. A. A. Earp, G. B. Smith, P. D. Swift, and J. Franklin, "Maximizing the light output of a luminescent solar concentrator," Solar Energy **76**, 655–667 (2004).
26. T. Ahn, R. O. Al-Kaysi, A. M. Muller, K. M. Wentz, and C. J. Bardeen, "Self-absorption correction for solid-state photoluminescence quantum yields obtained from integrating sphere measurements," Rev. Sci. Instrum. **78**, 086105 (2007).